Kovove Mater. 62 2024 197–209
DOI: 10.31577/km.2024.4.197

Evaluation of residual stress, surface hardness, roughness, and wear resistance of AZ31 in SMAT process using Taguchi analysis

Ali Kazemi, Ali Heidari*, Kamran Amini**, Farshid Aghadavoudi, Mohsen Loh-Mousavi

Department of Mechanical Engineering, Khomeinishahr Branch, Islamic Azad University, Khomeinishahr/Isfahan, Iran

Received 20 April 2024, received in revised form 16 May 2024, accepted 15 June 2024

Abstract

Surface Mechanical Attrition Treatment (SMAT) is one of the processes used to improve surface properties. In the present study, the effect of process parameters such as the diameter and number of shots, working height, and SMAT time on the residual stresses and the mechanical properties of the AZ31 magnesium alloy surface is investigated. This analysis was performed using *Minitab software*, experimental tests, Taguchi test design (array L9), and signal-to-noise analysis. In this research, investigating the microstructure using a scanning electron microscope (SEM), determining the phases and crystal structure using an X-ray diffraction (XRD) pattern, measuring the hardness of the samples using the Vickers method, and evaluating the wear behavior of the samples using the wear test method by peening on the disc were considered. Samples 1 and 3 had the minimum and maximum mass reduction, accompanied by a 32 and 57 % increase in wear resistance compared to the raw sample. By performing the SMAT process during the L9 experiments, the nanocrystallization of the grains caused a 35 and 46 % increase in the hardness of samples 1 and 3 with minimum and maximum hardness, and as a result, an increase of 32 and 57 % in wear resistance was seen compared to the raw sample. According to the results, time was considered the most important parameter of the process, and it affected the residual stress, surface hardness, and wear resistance by 63 and 64 %, respectively. This relates to the fineness of the grains on the surface and the microstrains created by the SMAT process.

K e y w o r d s: AZ31 alloy, surface mechanical attrition treatment, Taguchi approach, microstructures, compressive residual stress, hardness, roughness, wear resistance

1. Introduction

The SMAT process is a kind of cold work process in which the surface of the parts is vibrated with a continuous flow and at high speed by steel shots with a diameter of 1 to 8 mm by a vibrating source (electric motor or ultrasonic source), and then it collides with the sample surface as a result of hitting the wall of the chamber with a completely random direction. The speed of the shots is proportional to the vibration frequency and the distance between the surface of the sample and the shots in the range between 1 and 20 $\mathrm{m\,s^{-1}}$. Each of these shots causes residual compressive stresses by hitting the surface of the piece quickly and uniformly. Severe plastic deformations delay the initiation of crack growth due to the impact of shots and residual compressive stress created in that area and increase the fatigue life of the part [1]. Another effect of SMAT is a surface hardening process, which is caused by changes in the shape of the piece due to the impact of shots. This process improves the surface and increases the life of many metal parts and alloys, such as magnesium alloy. Due to proper casting and a higher strength-to-weight ratio, magnesium and its alloys have a low density (1.7–1.85 $\mathrm{g\,cm^{-3}}$), which is approximately 35 % less than that of aluminum, 65 % less than that of titanium and 77 % less than that of steel, and is still considered as one of the most important light metals [2]. AZ31 alloy is the most widely used magnesium alloy due to its strength, flexibility, and corrosion resistance properties. This metal and its alloys are used in various industries such as medi-

*Corresponding author: e-mail address: heidari@iaukhsh.ac.ir
**Corresponding author: e-mail address: amini@iaukhsh.ac.ir

cal equipment, transportation, military, and space [3]. In the SMAT process, influencing parameters such as the diameter and number of shots, the working height (the distance of the part from the vibrating source), and the duration of SMAT are effective in the creation of compressive residual stress and the mechanical properties of the surface, which researchers have investigated. Maleki et al. investigated the intensity and degree of shot peening (the number of multiple collisions of shots in one area of the surface) with the Almen test on the microstructure and mechanical properties of low-carbon steel. They demonstrated that increasing the amount of surface coating and the intensity of shot peening increases the fatigue life and nano hardness of the surface [4]. Xia et al. investigated the effect of SMAT on the surface of magnesium alloy. These researchers showed that after performing the SMAT process, the depth of the layer with nanostructure was 85 μm, and the average grain size was 42.7 nm on the AZ31 magnesium alloy. Also, the depth of the hardened layer was created under the influence of the process with a thickness of 600 μm, and after performing the mentioned process, the hardness increased from 85.7 to 130.8 HV, which also improved the wear [5]. Haghigi et al. studied the effect of shot peening duration on the microstructure and wear behavior of magnesium alloy. They demonstrated that the surface grain size of AZ31 alloy decreased from 520 Å in the raw sample to 160 Å in the shot-blasted sample during 80 min, and due to severe plastic deformation, grain shedding, and microstrains on the surface, the wear resistance increased [6]. Arifvianto et al. evaluated the effect of SMAT on the surface roughness of AISI 316L steel. The results showed that the microhardness of the surface increased after the SMAT process. They demonstrated that after the SMAT process, the surface hardness at a point 0.1 mm deep from the surface increased from 1.6 to 2.9 GPa [7]. Gallitelli et al. examined the difference between shot peening and the SMAT process; the surface roughness in the SMAT process is lower than shot peening, and the SMAT process has higher surface quality and hardness. Also, the residual stress created in the SMAT process is higher [8]. By investigating the effect of increasing the duration of shot peening on the wear resistance of the titanium alloy surface, Takesue et al. showed that increasing the duration of shot peening caused a 70 % increase in the wear resistance of the surface, which is due to the nano-crystallization of the grains and the creation of microstrain on the surface [9]. Hence, according to these studies in the SMAT process, the mechanical properties of the surface are improved due to severe plastic deformation, increasing the residual stress and creating a nanostructured layer on the surface. Previous research investigated one or two effective parameters in shot peening processes. In this research, to complete the previous studies, using experimental tests and design of L9 Taguchi array and signal-to-noise analysis, the effects of all SMAT process parameters such as shot diameter, shot number, working height, and shot peening duration on compressive residual stress, surface hardness, the surface roughness and wear created on the surface of magnesium alloy AZ31 are determined.

Table 1. Chemical composition of AZ31 alloy (wt.%)

Al	Zn	Mn	Ni	Mg
3.01	0.45	0.03	0.05	bal.

2. Materials and methods

2.1. Experimental method

In the present study, samples of AZ31 alloy were used according to the chemical composition of Table 1. After cutting, the samples were prepared in the form of discs with a diameter of 21 mm and a thickness of 3 mm by a gradual mechanical surface treatment device with a frequency of 50 Hz and shots made of carbon steel, and the effect of the parameters on the compressive residual stress and the mechanical properties of the surface were investigated.

2.2. The main parameters of the SMAT process

The main parameters of the SMAT process in this part include shot diameter (A), shot number (B),

Table 2. Variables and their levels used as input data in the Taguchi-base DOE

Levels	Factors			
	A Diameter of ball (mm)	B Number of balls	C Work height (mm)	D Time (min)
Level 1	1	4	10	10
Level 2	2	8	15	15
Level 3	3	12	20	20

Table 3. The L9 (4 factors and 3 levels) mixed level of Taguchi orthogonal array design

Experiment no.	Factors			
1	1	1	1	1
2	1	2	2	2
3	1	3	3	3
4	2	1	2	3
5	2	2	3	1
6	2	3	1	2
7	3	1	3	2
8	3	2	1	3
9	3	3	2	1

working height (distance of the part from the vibrating source) (C), and duration (D). These parameters were changed in three levels, according to Table 2.

2.3. Optimization of SMAT process parameters

The tests were performed using the L9 orthogonal arrangement based on the Taguchi method, and the test results were analyzed using *Minitab software*.

2.4. L9 orthogonal arrangement

The L9 orthogonal array is used in the current paper, and the laboratory parameters of this orthogonal array can be seen in Table 3. Laboratory data can be seen in Table 4.

2.5. Taguchi method for designing experiments

In this research, Taguchi test (4 factors with 3 levels) L9 was used. Figure 1 shows the L9 algorithm, which includes input and output variables. As can be seen in Table 4, the test parameters are shown for each of the 9 Taguchi tests.

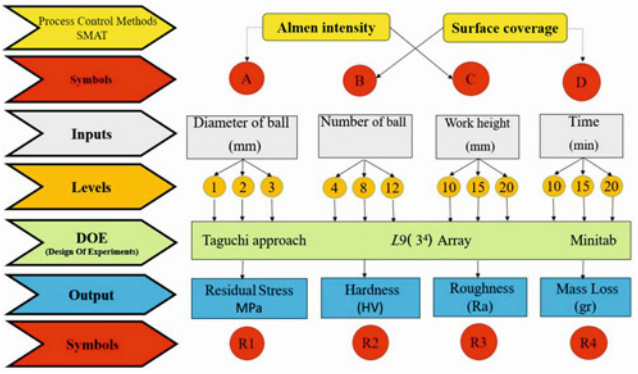

Fig. 1. Design of experiment based on the Taguchi method.

In this research, after the SMAT process of magnesium alloy AZ31, the samples have been examined and studied with the following tests:

(1) Investigation of the structure by X-ray diffraction analysis and scanning electron microscope.

(2) Examination of the residual stress and the amount of strains created on the surface by XRD.

(3) Measurement of the hardness of samples by Vickers hardness tester.

(4) Investigation of wear resistance and wear mechanism by wear test.

(5) Measurement of surface roughness.

2.6. Residual stress measurement

In the next step, XRD ASENWARE model AW-XDM300 was used with an X-ray wavelength of 1.54 Å and using the standard X-ray diffraction method and Bragg's law (Eq. (1)) for studying the structure and measuring the strain and residual stress created on

Table 4. Experimental layout after assigning the values of the parameters

	Inputs				Outputs			
Specimens No.	Diameter of ball A (mm)	Number of balls B	Work height C (mm)	Time D (min)	Compressive residual stress (MPa)	Hardness HV	Roughness (μm)	**Mass loss (g)**
1	1	4	10	10	105	100	1.4	**0.0046**
2	1	8	15	15	128	114	2.9	**0.0034**
3	1	12	20	20	152	125	4.2	**0.0029**
4	2	4	15	20	141	120	3.4	**0.0032**
5	2	8	20	10	115	105	1.7	**0.0045**
6	2	12	10	15	134	115	3.1	**0.0033**
7	3	4	20	15	125	112	2.6	**0.0040**
8	3	8	10	20	148	124	3.9	**0.0030**
9	3	12	15	10	122	110	2.3	**0.0042**
Raw (10)	–	–	–			68	1.1	**0.0068**

the surface [10]. X-rays were irradiated to the surface of the samples at a maximum penetration depth of 20 µm. X-rays have a certain wavelength, and any change in the distance between the crystal plates (d) leads to a shift in the angle of reflection (θ). Among the diffraction curves, the appropriate diffraction curve was selected in terms of the appropriate geometric shape to check the residual stress. Based on Bragg's law, Eq. (1), the distance between crystal plates is calculated in terms of θ (X-ray reflection angle), then by determining the position of the diffraction curve in each angle ψ (the angle between the vector perpendicular to the plane and the bisector of the projected and reflected angle), the graph $(d_\psi - d_0)/d_0$ in terms of $\sin(\psi)^2$ was drawn with angles ψ = –10, –20,–30, 0, 15, 30, 45 for all samples. According to the slope and intercept of the drawn lines and Eq. (1) [11], the residual stress on the surface of the magnesium alloy samples was calculated. The residual stress test was performed on a peak with an angle of $2\theta \cong 104.5°$, then the surface residual strain values were calculated according to the values of the compressive residual stress and the modulus of elasticity of the alloy. Also, the samples were phased using *Xpert high score software.*

$$\sigma_\Phi = \frac{E\,(d_\psi - d_0)}{(1+v)\,(\sin)^2\,\psi \times d_0}, \tag{1}$$

where σ_Φ represents the compressive residual stress, E is the modulus of elasticity, v is the Poisson coefficient, d_0 is the distance between crystal plates in angle ψ = 0, and d_ψ is the distance between crystal plates with the angle of ψ.

2.7. Microstructure analysis

The sample structure was investigated by SEM (VEGA-TESCAN-XMU). The grain size was calculated using the Scherrer equation and the X-ray diffraction pattern. Peak width in the X-ray diffraction pattern was half of the maximum height (Eq. (2)) [12]:

$$n\lambda = 2d\sin(\theta)\,. \tag{2}$$

Based on this equation, d is the distance between sequential atomic plates in a crystal network with respect to θ (the angle of X-ray emission to plates) and λ is the wavelength of X-ray:

$$d = \frac{0.9\lambda}{\beta\cos\theta}, \tag{3}$$

where d is the crystal size, λ is the X-ray wavelength, θ is the half of angle in the maximum height (rad), and β is the chosen peak width in the half of height in the diffraction pattern.

2.8. Investigating the sample's hardness

Hardness values were measured using an Innova model microhardness tester equipped with a Vickers indentation tool under a load of 300 grf. The microhardness values for the raw sample and 9 SMAT samples were calculated every 0.1 mm from the surface to a depth of 1000 µm (1 mm) on the magnesium alloy surface to evaluate the effect of SMAT on the microhardness.

2.9. Examining the wear behavior of the samples

The pin-on-disc method was used to check the wear behavior of the samples. The pin-on-disc wear test was performed with a force of 3 N and a speed of 0.2 m s^{-1} at a distance of 500 m on the surface. The wear mechanism of the samples was investigated with a field emission scanning electron microscope (FE-SEM, MIRA 3TESCAN-XMU model). Also, the mass reduction was reported every 100 m on the disc. The roughness (Ra) of the samples at a distance of 10 mm on the surface of the AZ31 alloy was measured using a digital surface roughness model, TIME 3200 (TR-200).

2.10. Statistical analysis

Taguchi method can be used to determine the optimal conditions. This variability can be expressed by the signal-to-noise ratio (the S/N ratio, denoted by η). The experimental condition with the maximum S/N ratio is considered optimal [13]. Experiments were conducted randomly based on the principles of Taguchi design. The objective function described in this research is to maximize residual stress and surface hardness and roughness. Therefore, the S/N ratio was calculated using the "the more, the better" approach. Equation (4) was used to calculate the S/N ratio [14]:

$$\eta = -10\log_{10}\frac{1}{n}\sum_{i=1}^{n}\frac{1}{y_i^2}, \tag{4}$$

where y_i is the value of the i^{th} response variable (residual stress, surface hardness, and roughness).

To minimize the reduced mass, the "the less, the better" approach was used to calculate the S/N ratio from Eq. (5) [15]:

$$\eta\ = -10\log_{10}\frac{1}{n}\sum_{i=1}^{n}y_i^2, \tag{5}$$

where y_i is the value of the i^{th} response variable (reduced mass).

Table 5. Response residual stress signal-to-noise ratios

Level	A	B	C	D
1	42.07	41.78	42.12	41.12
2	42.25	42.25	**42.29**	42.21
3	**42.36**	**42.64**	42.26	**43.34**
Delta	0.29	0.86	0.17	2.22
Rank	3	2	4	1

3. Results and discussion

By implementing the SMAT operation and applying the Taguchi L9 orthogonal array, it was demonstrated that the values of compressive residual stress and surface mechanical characteristics include roughness, hardness, and mass reduction, according to Table 4.

3.1. Residual stress

Residual stress was obtained using X-ray diffraction at a maximum penetration depth of 20 µm from the surface on the surface of 9 SMAT samples. The duration of the process is shown using Taguchi analysis in *Minitab software*. According to this figure, by using Taguchi analysis in *Minitab software*, the average values of residual stress in each of the levels of SMAT factors have been shown so that the difference in average residual stress for the process duration factor is more than for other factors, and this shows the greater impact of the parameter. Residual stress in the SMAT process is a result of the impact of the shot on the target surface, severe plastic deformation, and the creation of a nanostructured surface layer. Increasing the area of this surface increases its strength, and the optimal surface is obtained, so the signal-to-noise ratio is used as much as possible in residual stress analysis. As shown in Table 5, the optimal levels for residual stress with average and signal-to-noise ratio (S/N diagram) are shown. The values of optimal levels for residual stress $A3B3C2D3$ were obtained. The duration of shot peening and the number of shots are important coating factors. According to Figs. 2–4 and Table 5, the duration of the process has the greatest effect on the residual stress, and when the number of shots increases, more sequential collisions will occur, and there will be more coverage in the vicinity of the surface. The current findings are in good agreement with the research of Maleki et al., who showed that in the shot peening process, two factors determine the amount of shot coverage on the surface and the intensity of shot peening, the quality, and strength of the surface after shot peening. The coating factor has a greater effect on the residual stress than the intensity of shot peening [16].

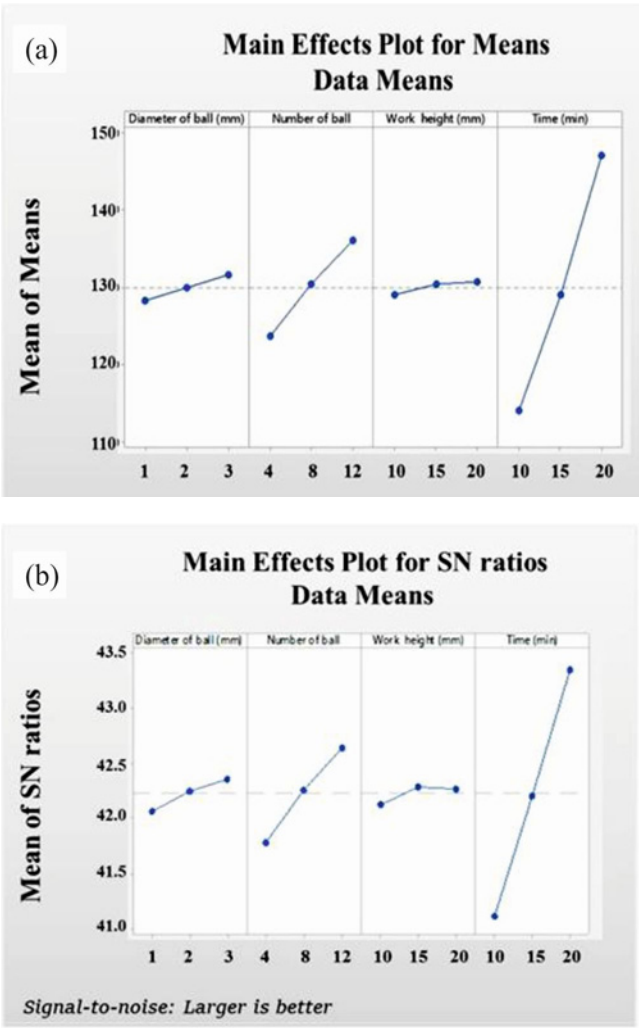

Fig. 2. Main effects plot for means (a) and S/N ratios (b) of compressive residual stress (MPa).

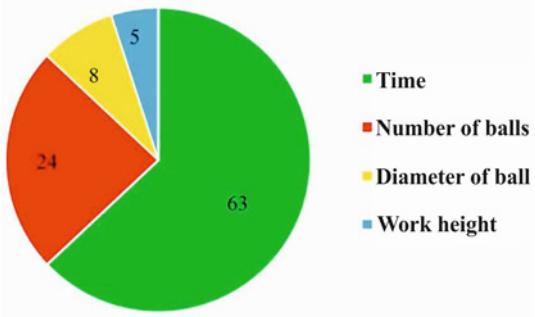

Fig. 3. Percentages of the influence of effective parameters on residual stress.

3.2. Examination of grain size and crystallites

The X-ray diffraction patterns for the raw magnesium alloy sample and 9 SMAT samples are presented

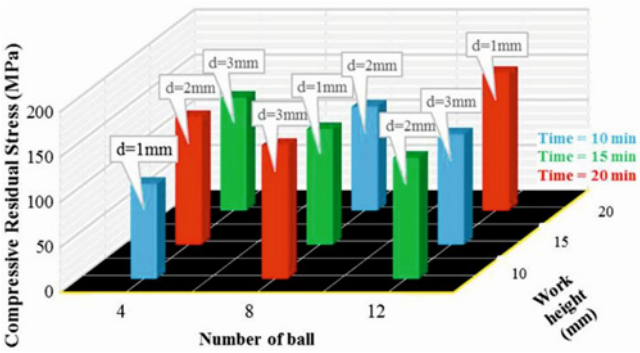

Fig. 4. Variation of residual stress with effective parameters.

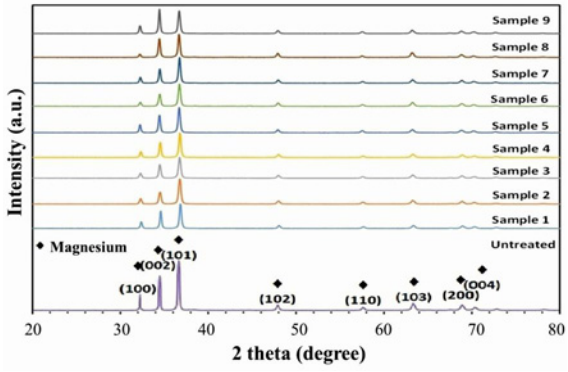

Fig. 5. XRD pattern of the raw sample and the samples after the SMAT process.

in Fig. 5. As it is seen, due to the SMAT operation, the peaks have been broadened, and the intensity of the peaks has decreased. This is because of the fineness of the grains and micro-strains that happened due to the impact of steel shots on the surface. In Table 6, the crystal sizes are extracted from the XRD data. Figure 6 shows the SEM images of the raw sample and SMAT samples No. 1 and 3. This figure shows the reduction of grains and deformed layers from the surface for samples 1 and 3, which have the minimum and maximum depth of deformation from the surface, compared to the raw sample. The size of the crystals in the non-SMAT sample is 139 nm, and in the SMAT samples, it is 103 and 81 nm for samples 1 and 3, respectively, which does not indicate a decrease in the size of the crystals compared to the SMAT sample. According to the above figure, it can be said that the fineness of the grains and the surface deformation of the magnesium alloy are due to the severe plastic deformation on the surface of the samples during the SMAT process. The researchers' results are in very good agreement with the experimental data. Hiwi et al. investigated the effect of SMAT operation on magnesium alloy nanostructure layers. They demonstrated

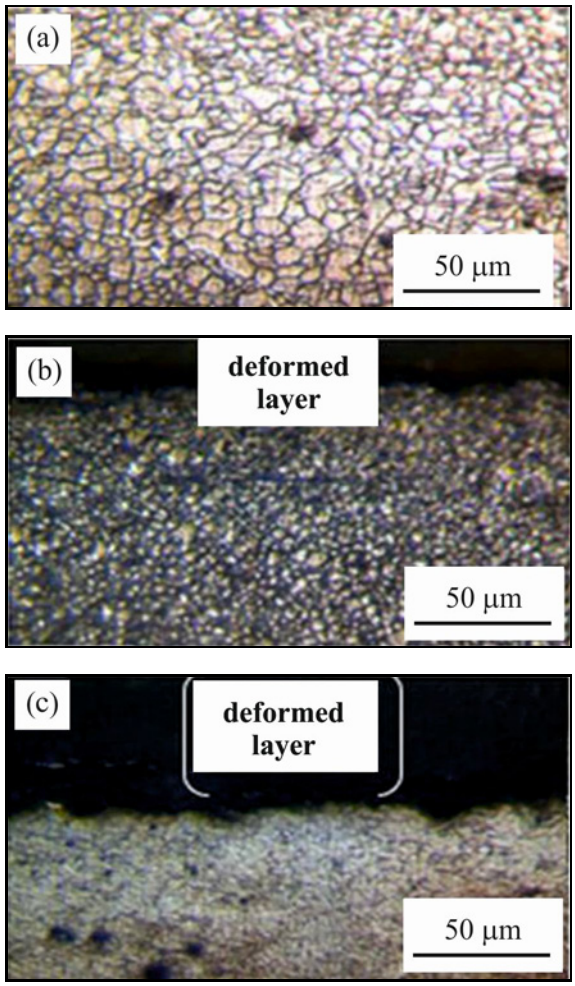

Fig. 6. SEM image for (a) as-received specimen microstructure SEM images, the effect of SMAT process on surface microstructures: (a) raw specimen, (b) specimen 1, and (c) specimen 3.

Table 6. Grain size of samples under SMAT operation

Sample	Crystallite size (nm)	Microstrain × 10^4
1	103	11.5
2	85	15.5
3	81	18.3
4	90	14.9
5	89	15.4
6	82	14.9
7	97	14.2
8	84	15.9
9	83	16.3
Raw	139	–

that nanocrystal layers were made on the surface of AZ91D alloy with a thickness of 10 µm and a grain size of 50 to 100 nm, and the thickness of 40 µm increased from 100 to 400 nm. Also, the hardness of the

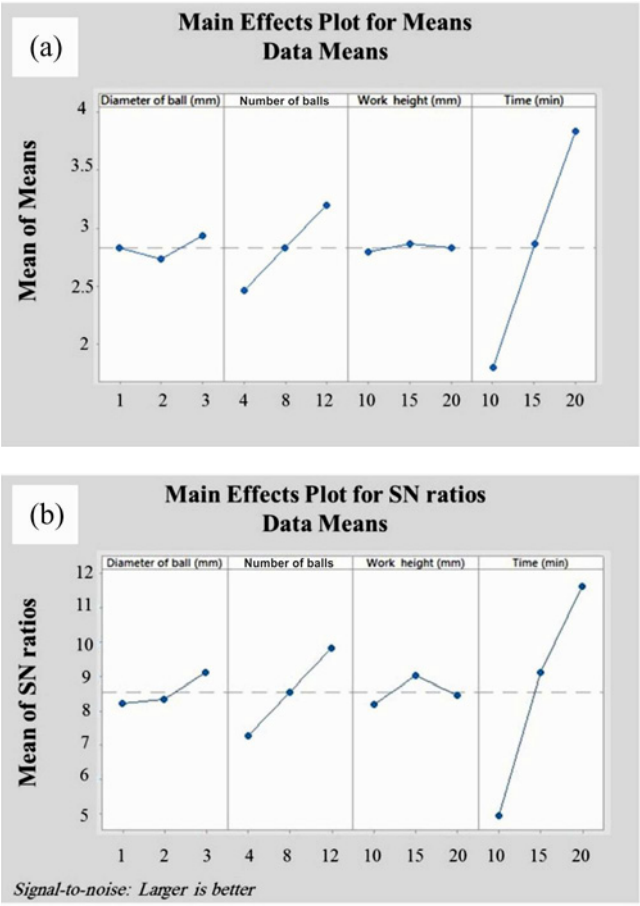

Fig. 7. Main effects plot for means (a) and S/N ratios (b) of hardness.

surface layers increased significantly after the process. The XRD results showed that due to the SMAT process, the height of the peaks became shorter and wider, and the diffraction intensity of the peaks was reduced. This is because of the fineness of grains and microstrains, which occurred due to the impact of steel shots on the surface and led to the improvement of mechanical properties [17].

3.3. Surface hardness

By performing the Vickers hardness test, the hardness of the raw sample was 68 HV. The values of surface hardness and depth of 1000 µm for 9 SMAT samples are shown. According to Fig. 7, in the *Minitab software*, the average hardness values of each level of the SMAT factors are shown, and the range of the average hardness difference for the factors of shot peening duration and number of shots is greater than other factors, which shows the greatest effect of these two factors on the surface hardness. Concerning the desirability of the surface hardness and strength, the signal-to-noise analysis was used. As shown in Table 7, the

Table 7. Response hardness signal-to-noise ratios

Level	A	B	C	D
1	41.03	40.86	41.03	40.42
2	41.07	41.14	**41.18**	41.11
3	**41.23**	**41.33**	41.12	**41.80**
Delta	0.20	0.47	0.15	1.38
Rank	3	2	4	1

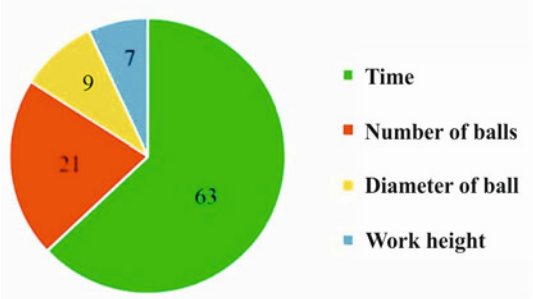

Fig. 8. Percentages of the influence of effective parameters on hardness.

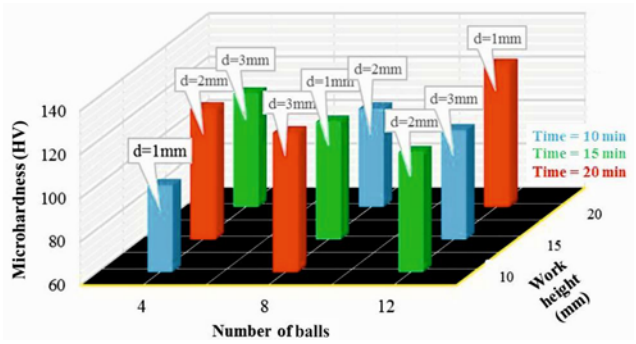

Fig. 9. Variation of hardness with effective parameters.

optimal surface values for $A3B3C2D3$ hardness were obtained. As it is known, shot peening time has the greatest effect on surface hardness, and the number of shots, shot diameter, and working height are in priorities 2, 3, and 4, respectively. Based on Fig. 8, the effect of each of the parameters of shot peening duration, shot number, shot diameter, and working height on surface hardness is 63, 21, 9, and 7 %, respectively.

Figure 9 shows the effect of different factors on compressive residual stress by calculating the average hardness of each factor for a specific surface. It is clear that the duration of shot peening has the greatest effect on the hardness value. The duration of shot peening and the number of shots are two important coating factors. Based on Figs. 7–9 and Table 5, the time and number of shots have the greatest effect on surface hardness. The current findings are in good agreement

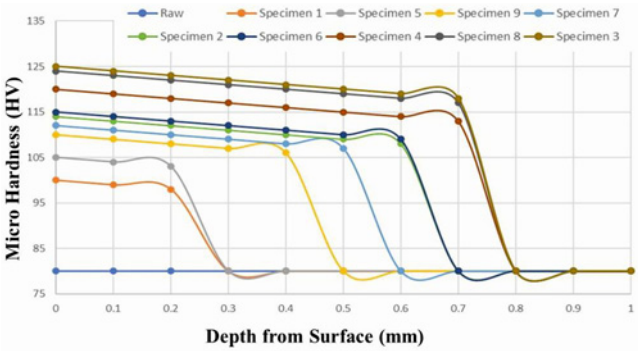

Fig. 10. Hardness of the raw sample and the samples after the SMAT process.

with Maleki et al.'s research, which investigated the effect of coating parameters and shot peening intensity on the grain size, residual stress, and surface hardness of AISI1016 alloy on the process of severe shot peening and conventional shot peening using Taguchi's L18. They reported that the impact of the shot peening parameter on grain size, residual stress, and surface hardness is greater than the shot peening intensity parameter [18].

Figure 10 shows the hardness values of the raw sample and 9 SMAT samples to a depth of 1000 µm from the magnesium alloy surface. The depth of the hardened area after the SMAT process was 200, 300, and 800 µm in different samples, respectively, and after this depth, the hardness of the lower layers decreases and reaches a constant amount, which equals the hardness of the surface without SMAT, which is consistent with the depth of the deformed layer (grain refinement) from the surface in Fig. 6. The hardness values of samples 1 and 3 increased by 47 and 83 %, respectively, compared to the raw sample, which is due to the creation of residual stress and strain, crushing and compression of grains on the magnesium alloy surface layer. The findings were in good agreement with the results of Zhou et al., who investigated the effect of ultrasonic shot peening duration on increasing the hardness of the titanium surface. The hardness of the surface increased by 75 % compared to the raw sample [19].

3.4. Surface roughness

According to Fig. 11, the average roughness values in each of the levels of the SMAT process factors are shown in the *Minitab software*, and the difference range of the average roughness for the factors of process duration and number of shots is greater than other factors, which demonstrates the greater effect of these two parameters on roughness. This is because of the mechanical hardening during the SMAT process using steel shots that randomly hit the surface, and with the fineness of the grains on the surface, creating residual stress and increasing the surface strength, roughness will increase. Although an excessive increase in roughness is not desirable, an increase in roughness is required for coating processes in the industry and creating a desirable final surface. It can also be used on implants in medical applications by creating a controlled interconnected porous structure to increase the biological interaction with the tissue or bone environment. Hence, the higher signal-to-noise ratio was used.

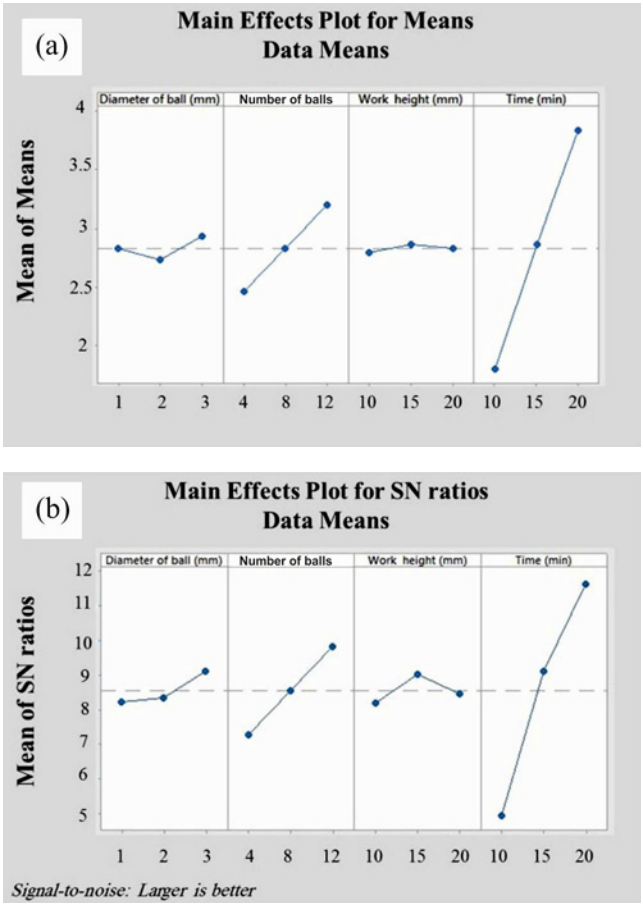

Fig. 11. Main effects plot for means (a) and S/N ratios (b) of roughness (µm).

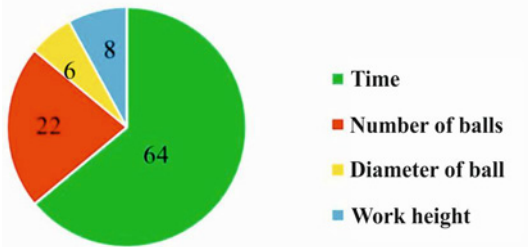

Fig. 12. Percentages of the influence of effective parameters on roughness.

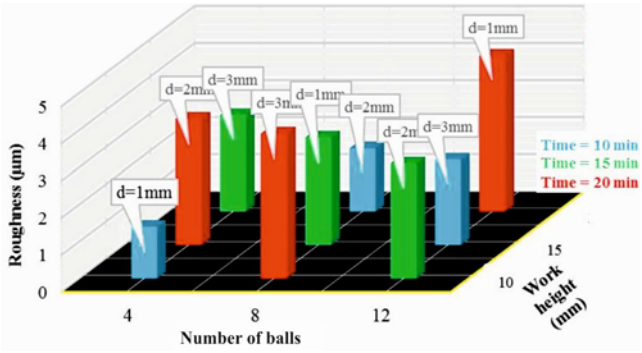

Fig. 13. Variation of roughness with effective parameters.

Table 8. Response roughness signal-to-noise ratios

Level	A	B	C	D
1	8.212	7.284	8.190	4.922
2	8.355	8.559	**9.037**	9.125
3	**9.118**	**9.842**	8.458	**11.639**
Delta	0.906	2. 558	0.847	6.717
Rank	3	2	4	1

Optimum stress levels for roughness are shown with mean and S/N ratio. The values of the optimal surface roughness $A3B3C2D3$ were obtained. According to Fig. 12, the effect of each process duration parameter, shot number, shot diameter, and working height on the surface roughness is shown, which is 8, 6, 22, and 64 %, respectively. In Fig. 13, the effect of different factors on the surface roughness is obtained by calculating the average roughness of each factor for a specific surface. The amount of participation and effectiveness of roughness for each factor is shown by calculating the maximum difference between the three levels of each factor for a desired result. As it is known, the roughness values are higher in the samples with the duration of the operation. This indicates the greater impact of the process duration than other surface roughness parameters. According to Figs. 11–13 and Table 8, the time and number of shots have the greatest effect on surface roughness. The results of this research are consistent with those obtained by Kumar et al., who studied the effect of time and pressure parameters on the surface roughness in titanium alloy by designing the Taguchi L16 orthogonal array test. Researchers showed that the effect of surface mechanical attrition treatment time as an important factor in the amount of coating on the surface is greater than other parameters on surface roughness [20].

Figure 14 shows the SEM images of the raw sample and the SMAT-treated samples 1 and 3 of magnesium alloys, with the minimum and maximum surface roughness values. By performing the SMAT operation

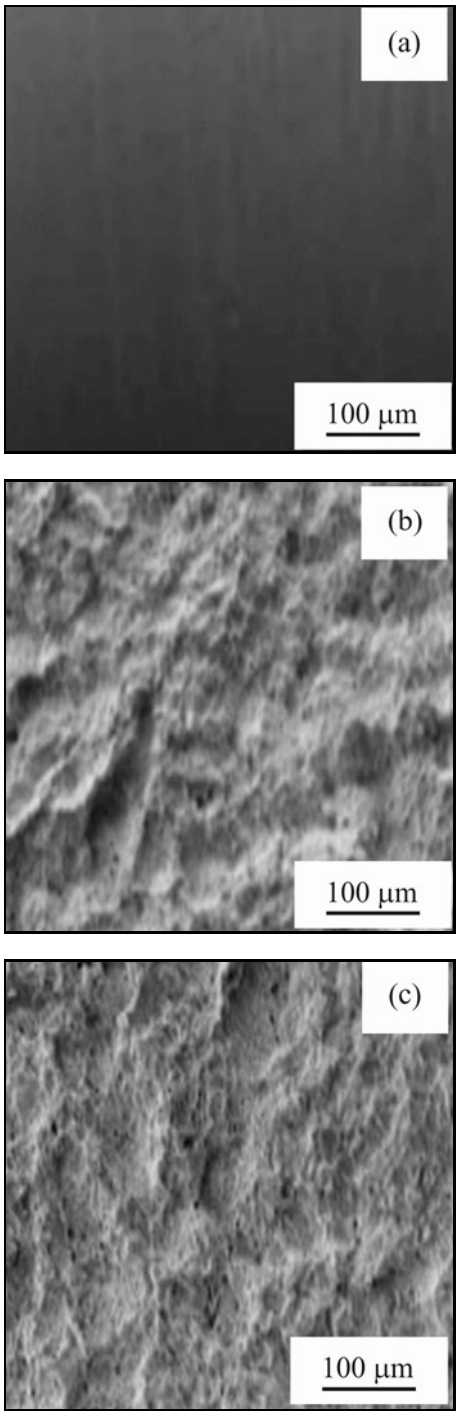

Fig. 14. SEM images, surface roughness for the raw and SMAT specimens: (a) raw specimen, (b) specimen 1, and (c) specimen 3.

due to the continuous impact of the shots on the surface and creating depressions and bumps on the surface of magnesium alloy, surface roughness increases.

According to Table 4, the surface roughness increased from 1.1 μm in the raw sample to 1.4 and 4.2 μm. The current findings are in good agreement

Table 9. Response mass loss signal-to-noise ratios

Level	A	B	C	D
1	48.96	**48.20**	48.99	**47.07**
2	48.82	48.92	48.93	48.99
3	**48.65**	49.31	**48.55**	50.37
Delta	0.31	1.11	0.38	3.30
Rank	4	2	3	1

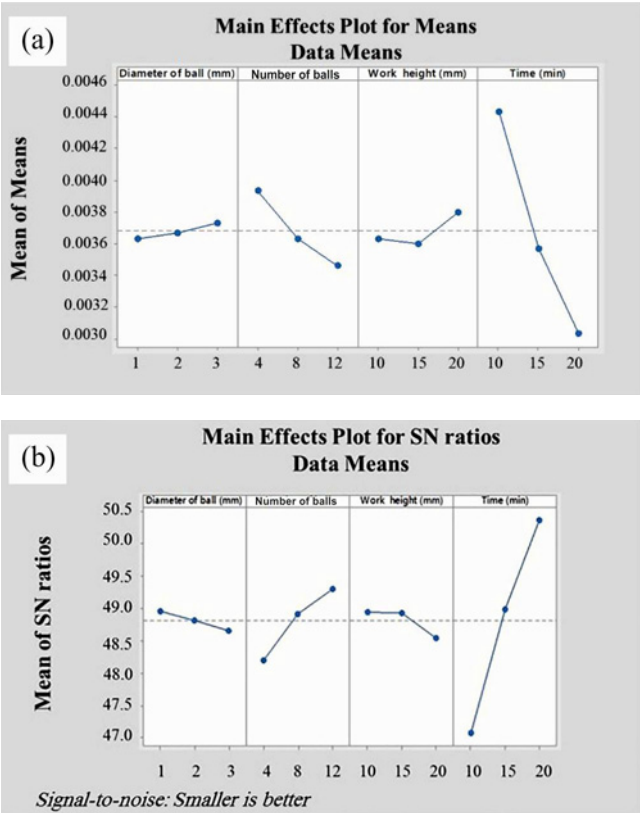

Fig. 15. Main effects plot for means (a) and S/N ratios (b) of mass loss (g).

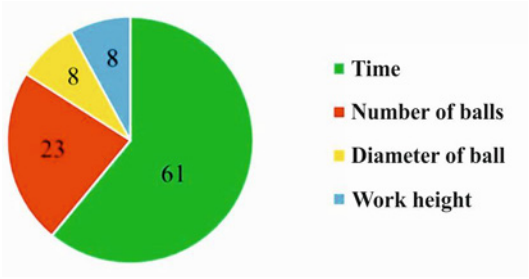

Fig. 16. Percentages of the influence of effective parameters on mass loss.

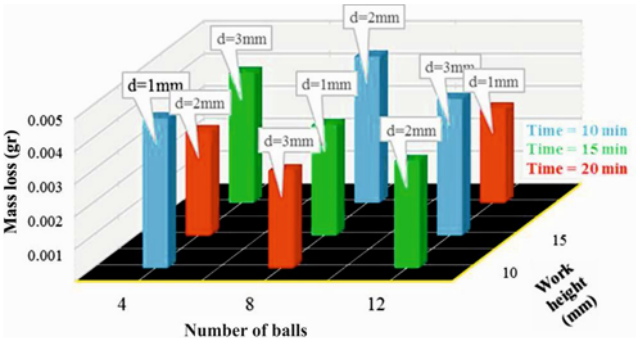

Fig. 17. Variation of mass loss with effective parameters.

with the results of Kumar et al., who examined the effect of shot peening pressure and time parameters on titanium alloy surface roughness using the L16 Taguchi array and signal-to-noise analysis. They reported that the effect of shot peening time on surface roughness is greater than that of other parameters [20].

3.5. Wear behavior of samples

Figure 15 in *Minitab software* shows the average values of mass reduction in each SMAT process factor level. It can be seen that the range of difference in the average mass reduction for factors of process duration and number of shots is greater than other factors, and the effect of these two parameters is higher on mass reduction. In the SMAT process, it is desirable to decrease the samples' mass and increase wear resistance. Therefore, the signal-to-noise ratio was used as low as possible. According to Table 9, the duration of the operation has the greatest effect on mass reduction. The optimal levels of mass reduction are indicated by the mean and S/N ratio. The values of optimal levels were obtained for reducing the mass of $A3B1C3D1$.

Figure 16 shows the effect of each parameter for shot number, impact time, working height, and shot diameter on mass reduction, which was 61, 23, 8, and 8 %, respectively. The mass reduction values of each sample in Fig. 17 demonstrate the effect of different factors on mass reduction, which is determined by calculating the average reduced mass related to each factor for a specific surface. The reduced mass effect of each factor is seen. Since the mass reduction values of samples with operation time are lower than those of

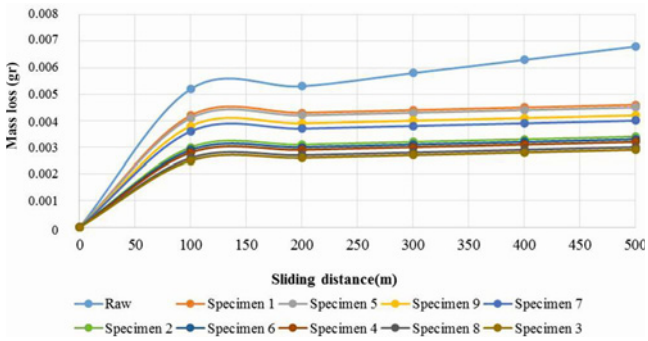

Fig. 18. Variation of mass loss with distance covered on the surface for raw and SMAT processed specimens.

other samples, the wear resistance is higher. This indicates that operation time affects mass reduction more than other factors. The findings have shown that the mass reduction values of the samples with a time of 20 min are more than those of other samples, indicating the greater effect of the processing time than other parameters on the surface roughness. The operation time and the number of shots are two key factors in the coating that increase the wear. The amount of mass reduction from the surface after SMAT operation is shown. According to Figs. 15–17 and Table 9, the time and number of shots had the greatest impact on mass reduction. The present findings are consistent with the study performed by Takesue et al., who studied the effect of the shot peening process on the wear resistance of titanium alloy surface [9].

After the SMAT operation and the pin-on-disc test on the raw and SMAT samples over a distance of 500 m on the magnesium alloy surface, the mass values reduced from the surface are shown in Fig. 18. As it is known, with increasing the area on the surface, the amount of mass reduction in the samples increases. Also, samples 1 and 3 have the minimum and maximum mass reduction, indicating a 32 and 57 % increase in wear resistance compared to the raw sample.

3.6. Wear mechanism

Figure 19 shows the wear mechanism of samples 1 and 3, which have minimum and maximum surface hardness. Adhesive and abrasive mechanisms can be seen on the surface of these samples. In addition, the adhesive wear was reduced by increasing the surface hardness in the SMAT process. Sample 3 has the lowest adhesive wear due to the greater hardness and depth in the deformed layer (granulation) compared to the magnesium alloy surface. In multi-layered or dispersed samples, adhesive wear is obvious. To investigate the wear mechanism further, the surfaces of the samples in two adhesive and non-adhesive areas

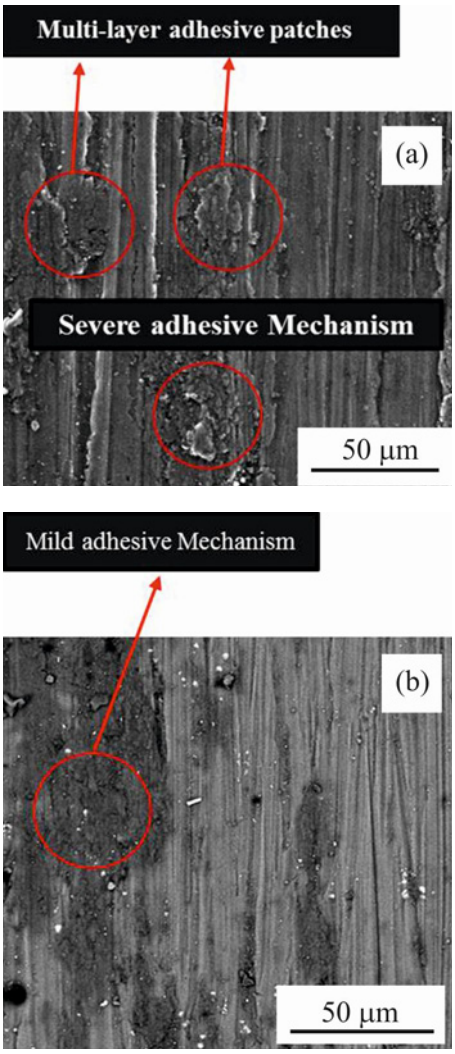

Fig. 19. SEM images of the wear surface in the SMAT sample: (a) sample 1, (b) sample 3.

(points B and A) were examined using an EDS analysis. As can be seen from Fig. 20, the amount of oxygen in the adhesive area is higher than in the non-adherent area (Fig. 20a in comparison with Fig. 20b). In the area with more hardness (sample 3), the adhesive wear is weaker, and in the area with lower hardness (sample 1), the adhesive wear is more. Hence, the chemical oxidation or turbo wear mechanism is also seen in the adhesive area due to more friction.

4. Conclusions

The SMAT process is a method to improve the mechanical surface properties due to severe plastic deformation, nanostructure, compressive residual stress, micro-strains, and fine grain on the surface. In this study, the effect of all parameters was investigated in the SMAT process on the compressive residual stress,

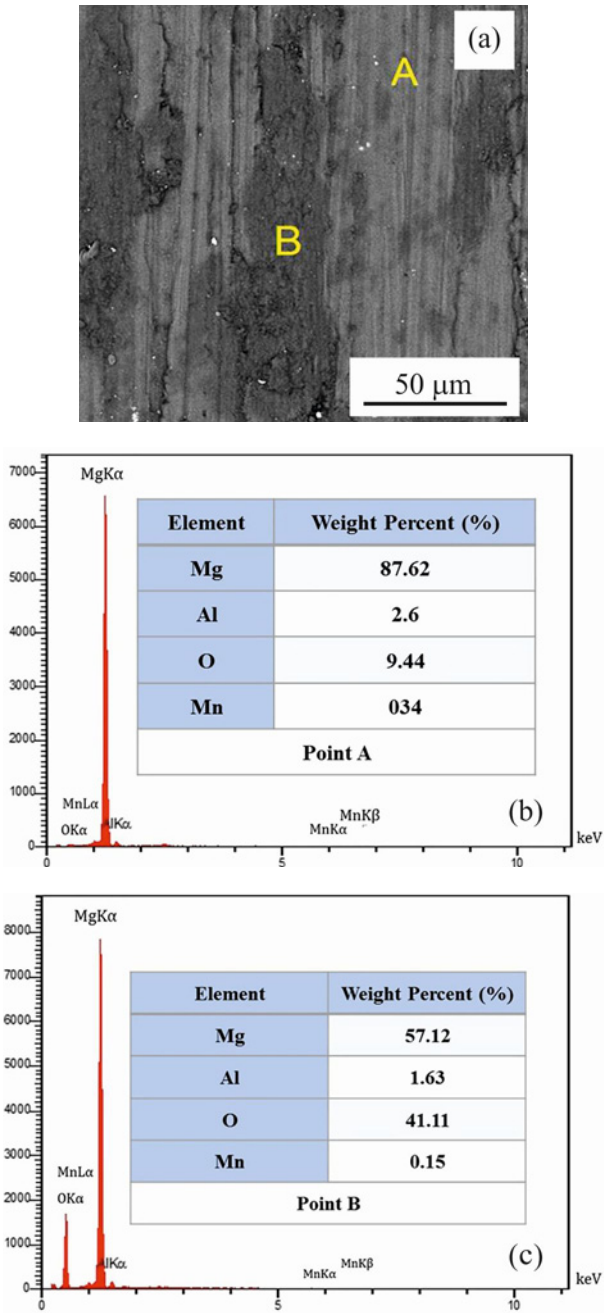

Fig. 20. Surfaces wear and EDS analysis SMAT processed specimen 3: (a) wear surface, (b) and (c) EDS analysis at points A and B.

hardness, wear resistance, and surface roughness of AZ31 alloy. Experimental tests, Taguchi L9 array test design, and signal-to-noise analysis were used for this purpose.

1. Among the effective parameters in the SMAT process, operation time was a key factor and affected the compressive residual stress, hardness, roughness, and wear resistance of magnesium alloy surface by 63, 63, 63, and 61 %, respectively.

2. The hardness of samples 1 and 3 (with minimum and maximum hardness) increased by 35 and 46 %, respectively, compared to the raw sample, which is due to severe plastic deformation, creation of nanostructures on the surface, compressive residual stress, microstrains, and grain crushing on the surface.

3. After the SMAT operation, the wear resistance of the SMAT samples 1 and 3 (with maximum and minimum mass reduction) increased by 32 and 57 %, respectively, compared to the raw sample.

4. The surface roughness of the SMAT samples increased compared to the raw sample due to the continuous impact of the shots and their random impact on the magnesium alloy surface.

5. Optimum levels for residual stress, hardness, roughness, and reduced mass are shown with average and signal-to-noise ratios (S/N graph). The values of optimal levels were obtained for residual stress $A3B3C2D3$, hardness $A3B3C2D3$, roughness $A3B3C2D3$, and wear behavior $A3B1C3D1$.

References

[1] M. Chemkhi, D. Retraint, A. Roos, C. Garnier, L. Waltz, C. Demangel, G. Proust, The effect of surface mechanical attrition treatment on low temperature plasma nitriding of an austenitic stainless steel, Surface and Coatings Technology 221 (2013) 191–195. https://doi.org/10.1016/j.surfcoat.2013.01.047

[2] M. Gupta, N. M. L. Sharon, Magnesium alloys and magnesium composites, John Wiley & Sons, Hoboken, 2011. ISBN: 978-0-470-49417-2

[3] N. Li, Y. Zheng, Novel magnesium alloys developed for biomedical application: A review, Journal of Materials Science & Technology 29 (2013) 489–502. https://doi.org/10.1016/j.jmst.2013.02.005

[4] E. Maleki, O. Unal, Fatigue limit prediction and analysis of nanostructured AISI 304 steel by severe shot peening via ANN, Engineering with Computers 37 (2021) 2663–2678. https://doi.org/10.1007/s00366-020-00964-6

[5] S. Xia, Y. Liu, D. Fu, B. Jin, J. Lu, Effect of surface mechanical attrition treatment on tribological behavior of the AZ31 alloy, Journal of Materials Science & Technology 32 (2016) 1245–1252. https://doi.org/10.1016/j.jmst.2016.05.018

[6] O. Haghighi, K. Amini, F. Gharavi, Effect of shot peening operation on the microstructure and wear behavior of AZ31 magnesium alloy, Protection of Metals and Physical Chemistry of Surfaces 56 (2020) 164–168. https://doi.org/10.1134/S2070205120010098

[7] B. Arifvianto, S. Suyitno, M. Mahardika, P. Dewo, P. T. Iswanto, U. A. Salim, Effect of surface mechanical attrition treatment (SMAT) on microhardness, surface roughness and wettability of AISI 316L, Materials Chemistry and Physics 125 (2011) 418–426. https://doi.org/10.1016/.2010.10.038

[8] D. Gallitelli, D. Retraint, E. Rouhaud, Comparison between conventional Shot Peening (SP) and Surface

Mechanical Attrition Treatment (SMAT) on a titanium alloy, Advanced Materials Research 996 (2014) 964–968. https://doi.org/10.4028/www.scientific.net/AMR.996.964

[9] S. Takesue, S. Kikuchi, H. Akebono, Y. Misaka, J. Komotori, Effect of pre-treatment with one particle peening on surface properties and wear resistance of gas blow induction heating nitrided titanium alloy, Surface and Coatings Technology 359 (2019) 476–484. https://doi.org/10.1016/j.surfcoat.2018.11.088

[10] P. Prevey, X-Ray Diffraction Residual Stress Techniques, Metals Handbook. American Society for Metals, Metals Park (1986) 380–392. https://doi.org/10.31399/asm.hb.v10.a0001761

[11] M. E. Fitzpatrick, A. T. Fry, P. Holdway, F. A. Kandil, J. Shackleton, L. Suominen, Determination of residual stresses by X-ray diffraction, Measurement Good Practice Guide 52, 2005.

[12] U. Holzwarth, N. Gibson, The Scherrer equation versus the Debye-Scherrer equation, Nature Nanotechnology 6 (2011) 534–534. http://doi.org/10.1038/nnano.2011.145

[13] A. Canakci, F. Erdemir, T. Varol, A. Patir, Determining the effect of process parameters on particle size in mechanical milling using the Taguchi method: Measurement and analysis, Measurement 46 (2013) 3532–3540. http://doi.org/10.1016/j.measurement.2013.06.035

[14] K. Li, S. Yan, Y. Zhong, W. Pan, G. Zhao, Multi-objective optimization of the fiber-reinforced composite injection molding process using Taguchi method, RSM, and NSGA-II, Simul. Model. Pract. Theory 91 (2019) 69–82. http://doi.org/10.1016/j.simpat.2018.09.003

[15] A. Qasim, S. Nisar, A. Shah, M. S. Khalid, M. A. Sheikh, Optimization of process parameters for machining of AISI-1045 steel using Taguchi design and ANOVA, Simul. Model. Pract. Theory 59 (2015) 36–51. http://doi.org/10.1016/j.simpat.2015.08.004

[16] E. Maleki, Modeling of severe shot peening effects to obtain nanocrystalline surface on cast iron using artificial neural network, Materials Today Proc. 3 (2016) 2197–2206. http://doi.org/10.1016/j.matpr.2016.04.126

[17] Y. Wei, B. Liu, L. Hou, B. Xu, G. Liu, Characterization and properties of nanocrystalline surface layer in Mg alloy induced by surface mechanical attrition treatment, Journal of Alloys and Compounds 452 (2008) 336–342. https://doi.org/10.1016/j.jallcom.2006.11.079

[18] E. Maleki, O. Unal, K. Reza Kashyzadeh, Efficiency analysis of shot peening parameters on variations of hardness, grain size and residual stress via Taguchi approach, Metals and Materials International 25 (2019) 1436–1447. https://doi.org/10.1007/s12540-019-00290-7

[19] K. Y. Zhu, A. Vassel, F. Brisset, K. Lu, J. Lu, Nanostructure formation mechanism of α-titanium using SMAT, Acta Materialia 52 (2004) 4101–4110. https://doi.org/10.1016/j.actamat.2004.05.023

[20] R. K. Kumar, P. Sampath Kumaran, S. Seetharamu, S. A. Kumar, T. Pramod, G. J. Naveen, Investigation of shot peening effect on titanium alloy affecting surface residual stress and roughness for aerospace applications, Procedia Structural Integrity 14 (2019) 134–141. https://doi.org/10.1016/j.prostr.2019.05.018